JOURNAL OF APPLIED POLYMER SCIENCE VOL. 8, PP. 151–167 (1964)

# Techniques for Studying Strain Rate Effects in Brittle Materials*

B. W. ABBOTT, R. H. CORNISH, and N. A. WEIL, *Armour Research Foundation, Illinois Institute of Technology, Chicago, Illinois*

## Synopsis

Techniques for studying brittle fracture over a strain rate range of $10^{-7}$–$10^{1}$ in./in./sec. and at temperatures from 75 to 1800°F are discussed. Techniques for achieving a uniaxial tensile stress in prismatic bars via a reflected stress wave method at strain rates up to $10^{3}$ in./in./sec. at room and elevated temperatures are presented. Results of the aforementioned effects in flexure, and experimental verification of the stress-time-position history for the stress wave loading technique are presented along with applicable theoretical explanations. Applications of the above techniques to a broader spectrum of brittle and semi-brittle materials are described.

## I. Introduction

The critical temperature-strength retention requirements of aerospace applications have stimulated extensive research into the mechanical and physical properties of many brittle materials. The interest in brittle ceramics has been predicated to a considerable extent on their excellent oxidation resistance and high temperature strength characteristics.

Since the optimization of structural components is a prerequisite in space flight vehicle design, much emphasis has been placed on the ultimate strength characteristics. Since ceramics exhibit tensile strengths which are substantially lower than their compressive strengths, the area of ultimate tensile strength behavior has been given considerable study, and a variety of techniques for determining the ultimate tensile strength of brittle materials have evolved. Unfortunately, many of these involve: (*a*) an analysis based on a complicated state of stress assumed to exist during the experiment; (*b*) a complex specimen geometry which is difficult and expensive to produce in large numbers; or (*c*) the assumption of applicability of standard methods, specimens, and procedures which have been used for ductile materials with considerable success. In studying strain rate effects in brittle materials one must contend with all of the difficulties inherent in static testing coupled with the added problems associated with maintaining a reliable state of dynamic stress.

* This study was sponsored by the Ceramics and Graphite Branch, Metals and Ceramics Laboratory, Materials Central, Aeronautical Systems Division of the Air Force Systems Command under Contract No. AF 33(616)-7465.

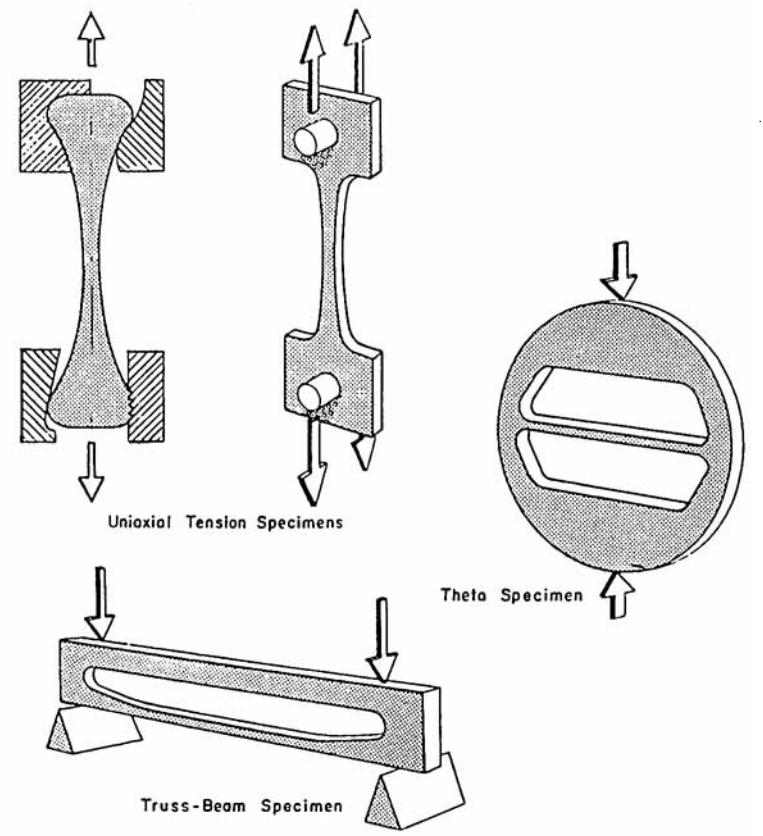


Fig. 1. Tensile tests for brittle materials.

Three common methods for evaluating the tensile strength of brittle materials are illustrated in Figure 1.

While the direct uniaxial tensile state of uniform stress provides simplicity of procedure and state of stress free from extraneous parameters, this technique does not appear to be applicable to brittle materials without introducing a considerable degree of sophistication into both the apparatus and procedures. Even when this can be done, extension of the technique to dynamic tests is not easily accomplished. In a ductile material under uniform tension the variation in stress across the cross section caused by an eccentricity of loading has a negligible influence on the ultimate strength. In this case the effects of bending cause a surface fiber to reach the yield point first and then upon yielding to transfer additional stress to adjacent fibers until the redistribution of stresses is obtained and the entire cross section is in a uniform state of stress. Since many brittle materials exhibit a linear stress-strain characteristic to failure, no yielding takes place, and hence, failure will occur whenever the maximum tensile strength is exceeded locally, even though a varying state of stress (caused by the superimposed effects of tension and flexure) is being maintained across the cross section.

Only very small eccentricities of load may result in substantial bending stresses leading to significant errors in strength determinations computed on the basis of average uniform stresses.

Additional methods using the "Theta"[1] specimen or "Truss-Beam"[2] specimen geometries provide a means for producing a state of tensile stress via a compressive ring and flexural specimen respectively. Both specimen geometries are sophisticated making specimens expensive in addition to which their applicability to many strain rates and temperatures is not yet clear.

Another technique, the SRI-NOL ring[3] has been used to study the ultimate tensile strength for a variety of materials. This method consists of internally pressurizing a thin ring of the material being considered. A rubber bag contained within the ring specimen and confining end plates is pressurized by hydraulic fluid. A simple pressure measurement allows an accurate strength determination for brittle materials from simple elastic theory provided the "thin-ring" geometry is maintained. With all its simplicity, this test does not appear to be readily adaptable to a broad range of strain rates or to elevated temperatures, hence was not applicable to this study.

Perhaps the simplest and most reliable test for ultimate strength studies over a broad spectrum of strain rates and temperatures is pure bending using a dogbone specimen. While this technique does not represent a pure state of stress it does produce a consistent tensile failure related to the uniaxial state of stress, and it possesses the advantages of having a well defined gage section which can easily be fitted to simple furnaces for elevated temperature studies. In this investigation such a method was used to study strain rate effects in magnesia, beryllia, and two kinds of alumina. Strain rates ranged from $10^{-7}$ to 10 in./in./sec., and from temperatures of 75 (nominal room temperature)–1800°F.

Another technique upon which initial work has been performed and is being developed for tensile strength studies at both room and elevated temperatures for strain rates of about $10^3$ in./in./sec. makes use of a reflected stress wave. In this method a compressive stress wave is generated in a long slender bar, and reflected from a free boundary as a pure tensile pulse. For brittle materials having a compressive strength far in excess of the tensile strength and a slender bar geometry, the extraneous effects of geometric dispersion, and attenuation are unimportant. As a result the traveling wave produces a transient state of pure stress which can be used to evaluate material properties free from eccentricity of loading and complexity of specimen geometry and test procedure.

## II. Dynamic Flexure Apparatus

The flexural apparatus used in this study was designed around the specimen configuration shown in Figure 2. The four-point bending apparatus was designed, built and modified to provide the most favorable condition of pure bending with a minimum of frictional constraint. Figure 3 shows a

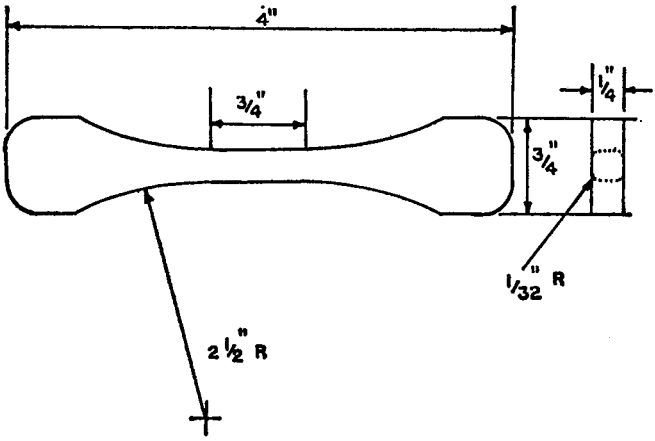


Fig. 2. Typical dogbone specimen.

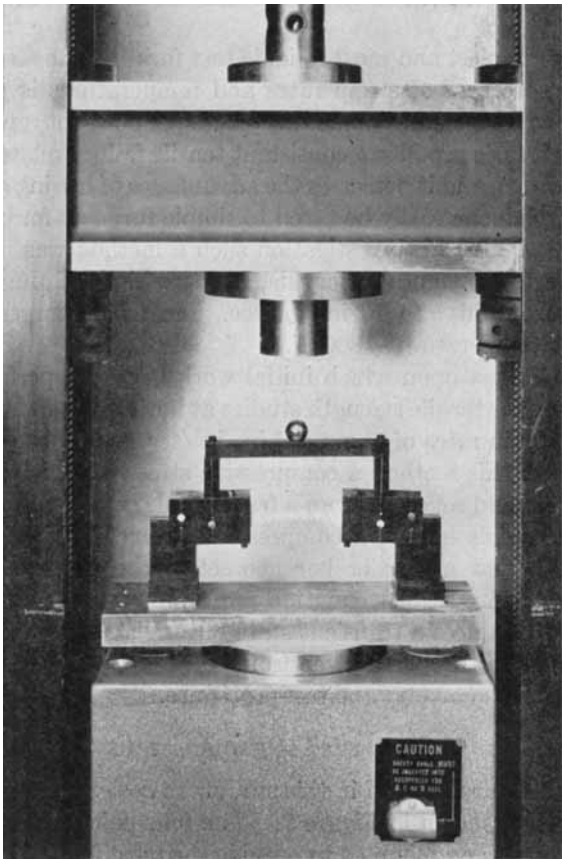


Fig. 3. Typical bending fixture.

typical bending fixture. The fixture consists of a pair of grips which attach to each end of the dogbone producing a variable section beam. Each grip contains two pins, one of which provides a loading point and the other a support point. In the resulting four-point loading system, the entire active portion of the specimen is in a region of constant bending moment. This puts the uniform reduced section of the dogbone in a state of pure bending. Care was taken to locate the pins so that the active contacting surfaces were all on the nominal neutral axis of the specimen. In addition to this, the pins were free to roll, thereby eliminating any friction contributing to the bending moment or induction of a net frictional tensile stress across the specimen cross section. One end of the load bar and one of the support pads contain pins perpendicular to grip pins.

This assures point contacts at one end of both the loading bar and the support. This feature prevents the development of torsional stresses about the longitudinal axis of the dogbone since the fixture cannot support a torsional moment around this axis.

The above apparatus type (several of which were built) was used over the entire spectrum of strain rates and temperatures. For strain rates from $5 \times 10^{-7}$ to $1 \times 10^{-2}$/sec., the apparatus was loaded in Riehle and Instron universal testing machines. Loading rates were varied from 0.0005 in./min. of crosshead motion to 20 in./min. For strain rates above $10^{-2}$, a falling weight was used with the same bend fixture. Essentially, this apparatus consisted of a guide tube in which a weight was dropped from a prescribed height onto a loading ball at the center of the load bar. This impact can be controlled well enough to apply a reproducible load pulse giving a state of dynamic bending.

## III. Measurement of Failure Loads and Strain Rates

As discussed, the mounted specimen is in a region of constant bending moment as long as the symmetry of the loading system is maintained. The symmetry condition was verified early in the bend test program; thereafter, a section of constant bending moment was assumed to exist for all tests since care was taken to maintain the symmetry of loading in each experiment.

In tests of this type on a brittle material, the total failure load and time to failure are the only quantities needed to compute the failure stress and strain rate. The bending moment over the gage section can be computed directly from the total load, and the failure stress determined from the bending moment and the section modulus at the failure section. To compute the strain rate it was necessary to determine the time to failure and to assume a value for the modulus of elasticity of the material at the temperature in question.

Early in the bend test program modulus of elasticity determinations at room temperature were made for the aluminas, and magnesia. For the drop tests at room temperature these measured modulus values were used to compute the failure stress from recorded values of dynamic strain. For

the lower strain rates in which the load (stress) was recorded, these moduli were used to compute the effective strain rates.

Elastic modulus values at elevated temperatures were obtained from the literature,[4] and used to compute effective strain rates from load-time records. It should be pointed out that this procedure is sufficiently accurate for strain rate determinations at high temperatures because the final plots of failure stress versus log strain rate are quite insensitive to comparatively large percentage errors in the strain rate. The effect of a small percentage error in the modulus is to shift the log strain rate values horizontally only a slight amount, hence it is of only minor importance.

For strain rates from $10^{-7}$ to $10^{-4}$ sec.$^{-1}$, the measurement of failure load and time to failure by conventional means (chart records or load dial plus stop-watch) is acceptable over the whole temperature range. For strain rates of $10^{-3}$–$10^{2}$/sec. the response of the system precludes the use of static recording and dynamic recording is required. All the recording in this regime was accomplished using a cathode ray oscilloscope with the load on the $y$ axis and time following a trigger signal (on pulse rise) on the $x$ axis. A Polaroid back scope camera was used to record the load-time trace. Load was transduced by a load cell and strain indicator demodulated and low band pass filtered for oscilloscope presentation.

Because of the difficulties encountered in attempting to measure load

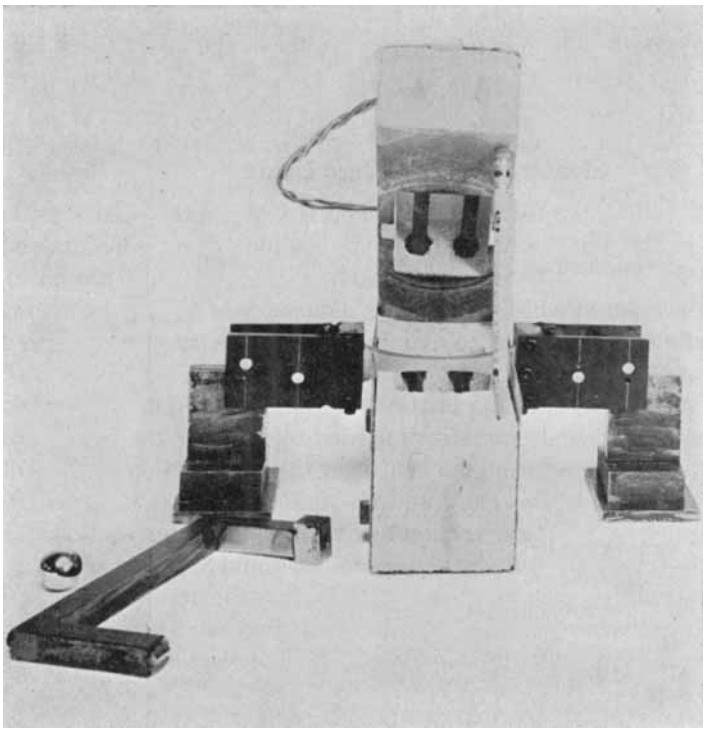

Fig. 4. Fixture and furnace—open condition.

with force transducers at the highest strain rate (drop test), specimens at room temperature were individually instrumented with etched foil resistance strain gages mounted on the tensile face. Each strain gage was used as an active element in a four-arm d-c bridge. Strain pulses were recorded by oscilloscope photography, sweep being triggered by a microswitch contacted by the falling weight. This procedure requires that failure strength be computed from the known moduli at each temperature as discussed earlier. Extension of this technique to higher temperatures (1000 and 1800°F.) was not successful.

## IV. Elevated Temperature Furnace

A furnace was designed around four silicon carbide "Glo-bar*" heating elements mounted in a firebrick. This furnace was found to be satisfactory with regard to temperature gradient along the gage section, and also possessed overall ruggedness and reliability. A photograph of the furnace in the opened condition is shown in Figure 4. The furnace is built in two notched halves to permit rapid specimen insertion and to cut down on overall testing time. In the machine tests it was possible to attach the upper section of the furnace to the moving cross head, so that after a specimen is broken and the cross head raised to insert a new specimen, the furnace is opened automatically. A plot of the temperature over the specimen gage length at a nominal temperature of 1800°F. is given in Figure 5.

## V. Experiments and Results in Flexure

Using the bend apparatus and range of strain rates mentioned in earlier sections, flexural experiments were carried out at nominal room temperature (75), 1000, and 1800°F. on Wesgo AL995 alumina, Lucalox alumina, ARF manufactured magnesia, and Atomics International beryllia. Between 8 and 20 specimens were tested at each of the strain rates studied for any particular test temperature.

The results of the experiments are shown in Figures 6, 7, 8, and 9. In these figures the average flexural stress at failure (modulus of rupture) is plotted against the log of the strain rate. The scatter band for each group is indicated by showing one standard deviation above and below the plotted point. These data have been subjected to a linear least squares analysis to arrive at the failure stress versus log of strain rate plots shown in Figures 6 through 9 and represented by the equation

$$\sigma_F = \sigma_0 + \sigma_1 \operatorname{Log}_{10}\left(\frac{\dot{\epsilon}}{\dot{\epsilon}_o}\right) \tag{1}$$

where $\sigma_F$ is the failure stress, $\dot{\epsilon}$ is the strain rate, $\sigma_0$ is the value of failure stress at a strain rate of $\dot{\epsilon}_o$, and $\sigma_1$ is the derived slope.

Since the lowest experimental strain rate was on the order of $10^{-7}$ sec.$^{-1}$

* Trade Name: The Carborundum Corporation.

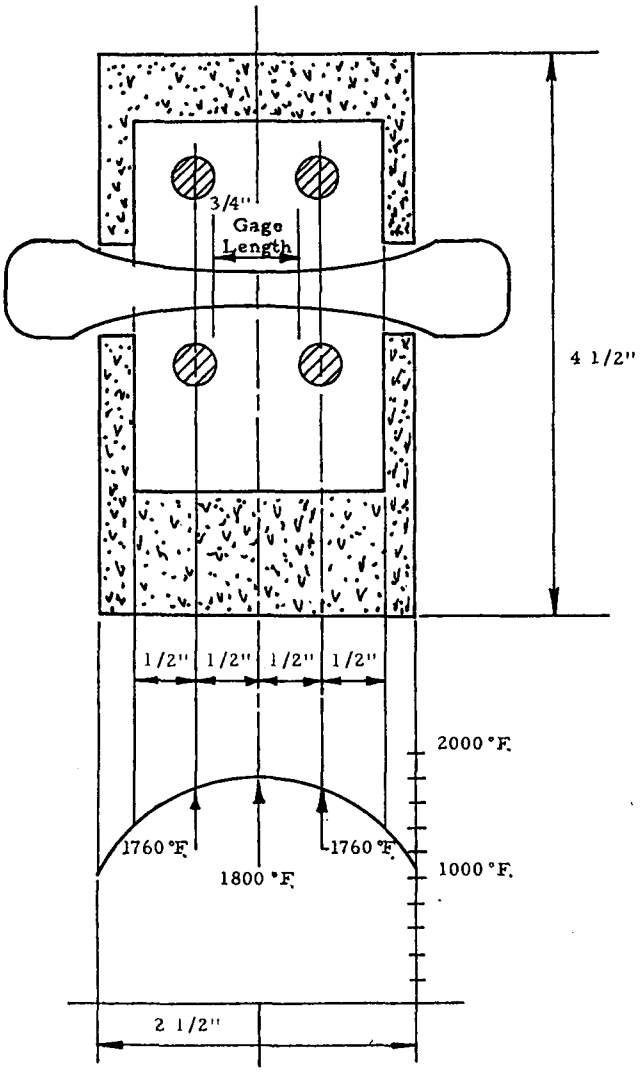


Fig. 5. Temperature gradient in center section of Glo-Bar furnace at 1800°F.

$\dot{\epsilon}_0$ was taken to be $10^{-7}$. This normalization is arbitrary and does not change the least squares fitted line, but only the form of the equation.

At the present condition of data density this linear relationship appears to represent the most realistic fit to the experimental data points obtained. As more points are added either by extension of the strain rate range or by filling in of the existing strain rate spectrum, a refinement for curves of a higher complexity than the simple semi-logarithmic linearity may become appropriate.

The results at room temperature do not appear to indicate any significant strengthening effect of strain rate. While the Wesgo alumina actually

shows a decrease in strength with increasing strain rate at room temperature the change is small enough that it may be of no significance.

At elevated temperatures the aluminas show substantial increases in strength with increasing strain rate. These results may be indicative of

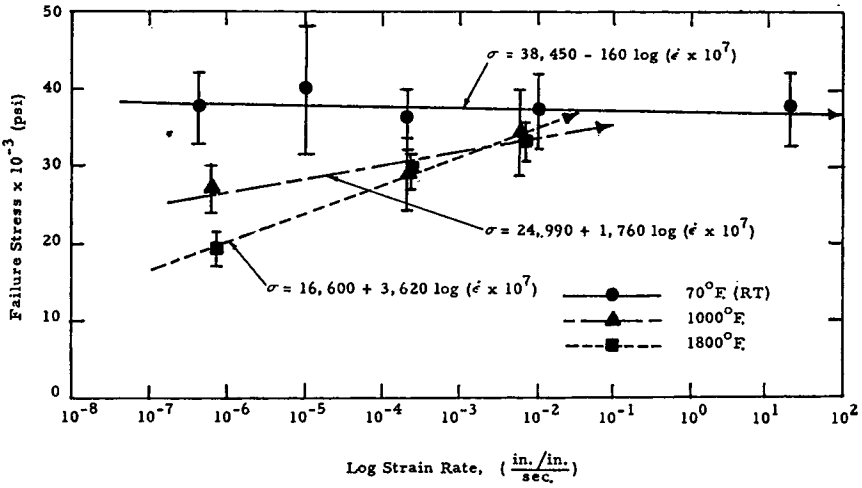


Fig. 6. Failure stress versus strain rate—Wesgo AL-995.

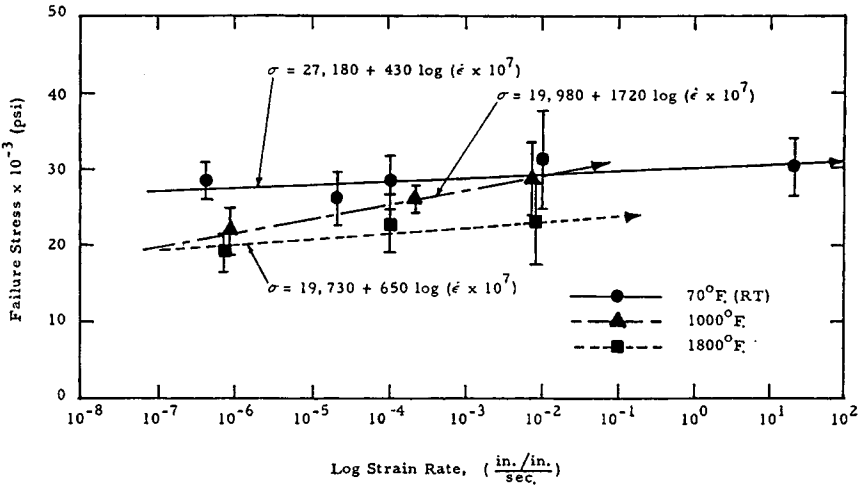


Fig. 7. Failure stress versus strain rate—Lucalox.

some microplasticity effects, although other investigations[5,6] have shown that such effects only initiate at temperatures of about 1800°F. While additional studies are needed to rigorously define the strength dependence on strain rate and temperature, the data of this investigation indicate a strengthening effect at elevated temperatures.

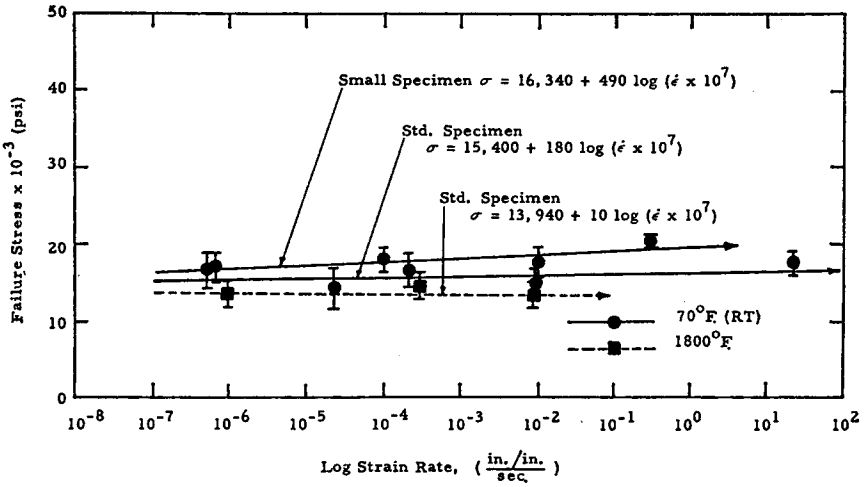


Fig. 8. Failure stress versus strain rate—magnesium oxide.

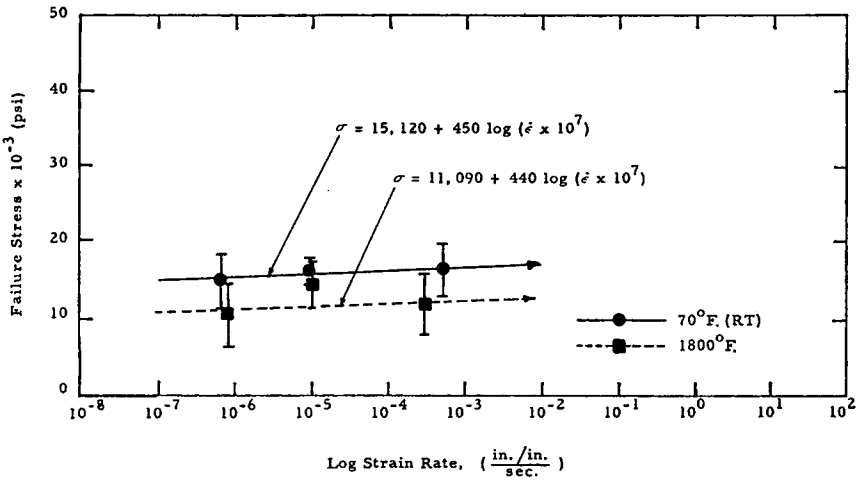


Fig. 9. Failure stress versus strain rate—beryllium oxide.

Neither magnesia nor beryllia show any significant strength variation with either strain rate or temperature increases. These data appear to agree with unpublished results of another study now in progress.

## VI. A Stress Wave Technique for Studying Tensile Strength

The stress wave technique provides a means of studying tensile strength under the action of a pure state of stress; which is rarely accomplished in many of the standard tensile tests for brittle materials. If (as the room temperature results in flexure in this investigation indicate) there is no significant strain rate effect in some ceramics at room temperature, then the tensile strength will be independent of the rate of loading; and the

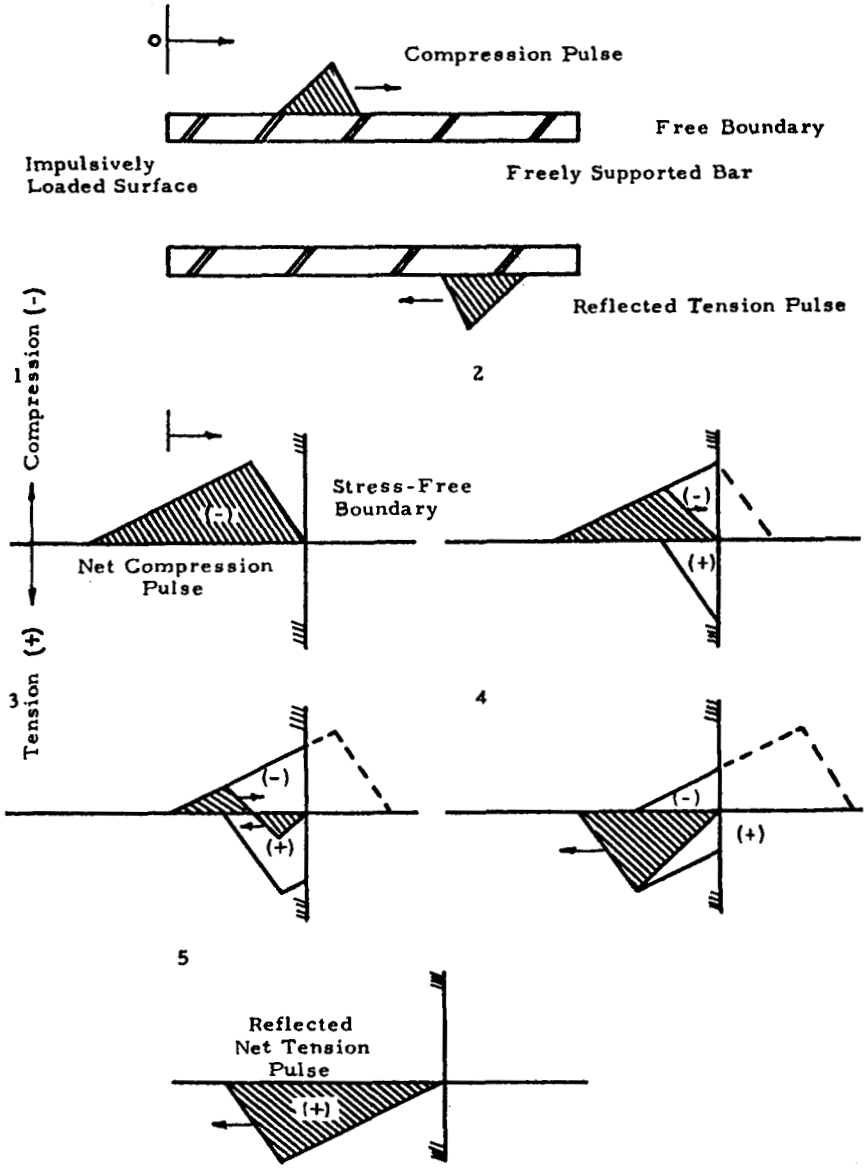


Fig. 10. Stress wave reflection from a free boundary.

stress wave technique can provide a standard tensile test for those materials. In the case where strain rate effects are significant such a method can provide strength data at strain rates far in excess of those provided by conventional methods.

The basis for the stress wave technique lies in the phenomena of normal reflection of a longitudinal wave from a free boundary. A nondispersing, non-attenuating traveling stress wave will be completely reflected from a

free boundary as a mirror image of the incident wave (i.e., a compression wave reflects as a tensile wave). Suppose an impulse is applied to one end of a freely supported slender* rod made of a material which is linearly elastic to failure.

In this case the initial compressive stress wave, starting at the impulsively loaded end will travel unattenuated down the length of the bar and be reflected as a mirror image tensile wave traveling in the opposite direction. The phenomena of stress wave reflection from a free boundary is illustrated schematically in Figure 10.

Since the compressive strength of most brittle materials greatly exceeds the tensile strength, the incident compressive pulse will not be of sufficient magnitude to cause a compressive failure in the bar as the wave travels toward the free end. However, the mirror image tensile wave generated at the free end upon reflection will be large enough to exceed the tensile strength, and a piece of the bar near the end will break off; provided the magnitude of the initial impulse is designed to exceed the ultimate tensile strength.

The one-dimensional theory of longitudinal stress waves is presented by Timoshenko[7] and Kolsky[8] and will not be reiterated here. By assuming that all cross sections remain plane during deformation, and neglecting the effects of lateral inertia it can be shown that:

$$\sigma = \rho c \frac{\partial \mu}{\partial t} \tag{2}$$

where: $\mu$ is the longitudinal displacement of an interior cross section which is $f(x,t)$ ($x$ denotes position and $t$ denotes time); $c$ is the velocity of propagation which is $\sqrt{E/\rho}$; $E$ is the modulus of elasticity; and $\rho$ is the mass density.

The incident compressive wave at the free end of the bar can be expressed in terms of the displacement of the free end as:

$$\sigma_c(L) = \frac{1}{2} \rho c \left.\frac{d\mu}{dt}\right|_{x=L} \tag{3}$$

The factor of $1/2$ comes from the fact that the particle velocity at the free end of the bar (due to the superimposed effects of incident compression and reflected tension) is twice as large as that of an interior section. Hence the stress in the bar as a function of time can be determined by transducing the velocity of the end of the bar during the reflection process.

The tensile strength of the material at the failure section can be determined if the following items are known: ($a$)the complete stress-time history of the incident compression wave; and ($b$) the position of the wave on the bar at the time of fracture.

* Slender refers to the fact that the lateral dimension of the bar must be small ($1/5$–$1/10$) compared to the wavelength of the stress wave or geometric dispersion of the wave will occur.

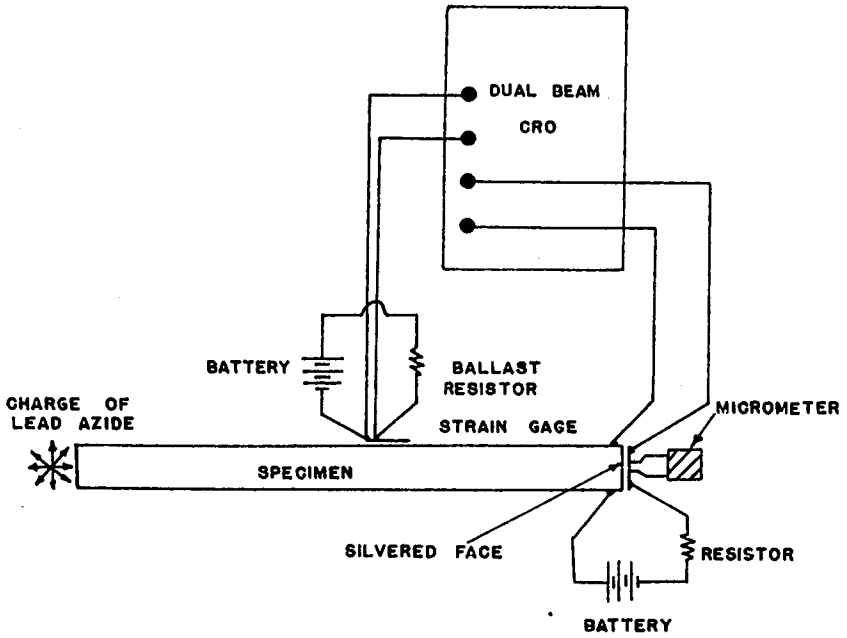


Fig. 11. Room temperature tensile strength determination setup for ceramic specimens.

Such a determination tacitly assumes the simple one-dimensional theory applies, and that the effects of dispersion and attenuation are negligible.

This being the case a relatively simple experimental setup is required to produce the data at room temperature. Such a setup is illustrated in Figure 11. The free end of the bar is silvered and used as one plate of a parallel plate capacitor. This device transduces the displacement of the end of the bar by sensing the gap change in the capacitor.

Strain gages mounted on the specimen can be used to determine the stress-time pulse on the surface of the bar. Presumably, this pulse will be uniform across the cross section of the bar provided that the bar is slender and the Poisson effect is small. In any case a comparison of the stress pulses obtained from strain gages with those resulting from monitoring the free end displacement will provide a means of determining the uniformity of stress across the cross section at any particular time. In addition, strain gages can be used to determine the position of the pulse on the bar at any particular time. By placing the gages less than one wavelength apart, some gages will necessarily be under strain at any particular time as the wave propagates down the bar.

The schematic in Figure 11 illustrates the practical components needed for performing the experiment. The impulse is supplied by an explosive charge of lead azide ignited by a piece of nichrome wire and a battery. The strain gage is shown as one leg of a potentiometric circuit. An oscilloscope with a polaroid scope back camera is used to monitor the transducers.

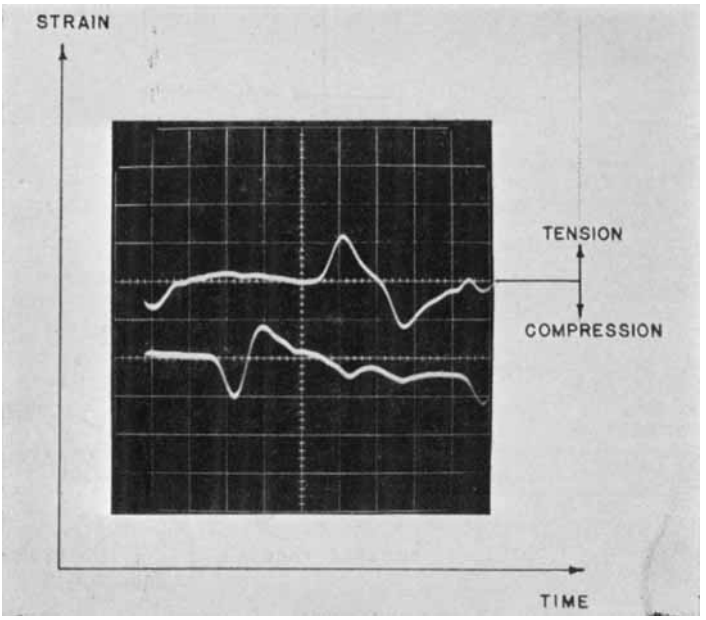


Fig. 12. A strain gage transduced stress wave: $C$ = velocity of propagation = 390,000 in./sec.; $T$ = period — 16 $\mu$sec.; $\lambda$ = wavelength = $CT$ — 6.25 in.; $d$ = lateral dimension of the bar = $^1/_4$ in., and $\lambda/d$ = 25.

Preliminary results of a study now in progress at ARF are shown in Figure 12. In this case a square bar ($^1/_4 \times {}^1/_4$ in.) of Wesgo AL995 aluminum oxide was instrumented with two foil type strain gages; one mounted near the center of the bar, and the other near the free end. The top trace represents the gage nearest the explosive charge. The traces move from left to right on the photograph. The first pulse on the top trace shows a portion of the incident compressive wave. The early portion of this pulse was used to trigger the oscilloscope. The lower trace then shows the incident compression pulse followed immediately by the reflected tensile pulse. These incident and reflected pulses are not of the same shape and magnitude because the second gage was so close to the free end that only the net wave at that station during reflection is recorded. The upper trace then shows the complete tensile pulse followed by a mirror image compression pulse which travels down the bar for the second time. The photograph indicates clearly that the effects of attenuation are absent, but the distortions shown on the latter portion of the lower trace are probably caused by a combination of electrical noise, shear waves, and dispersion effects. This fact will become clearer when the results obtained by using bars of smaller cross sections are available.

In a similar study by Kolsky[9] the same technique was used to study the failure strengths of glass and plastics. As in the current ARF study, Kolsky noted a clean break across the failure section. Kolsky also noted that the broken end pieces were close to one-quarter of a wavelength long

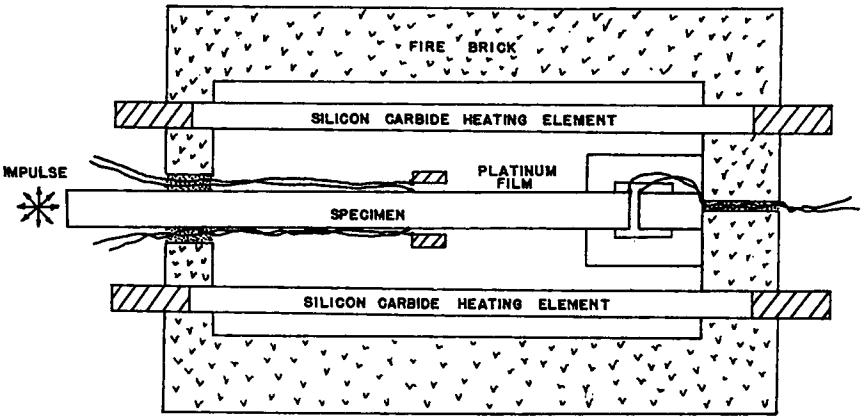


Fig. 13. Elevated temperature tensile strength determination setup for ceramic specimens.

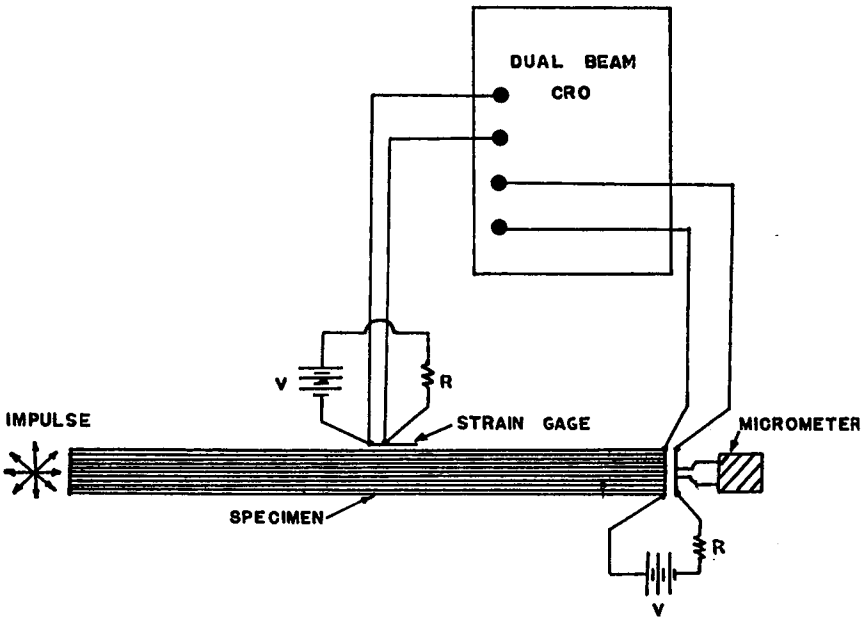


Fig. 14. Glass reinforced plastic specimen configuration.

and therefore found failure to be occurring on the peak of the tensile pulse. For brittle materials, such as ceramics which have significant strength differences from specimen to specimen, failure on the pulse maximum could only be obtained through a succession of increasing stress pulses. Since such a technique may produce cumulative damage to the specimen, erroneous strengths would be obtained. Hence while a maximum pulse approach requires less data for a strength determination, it may not be applicable to all brittle materials.

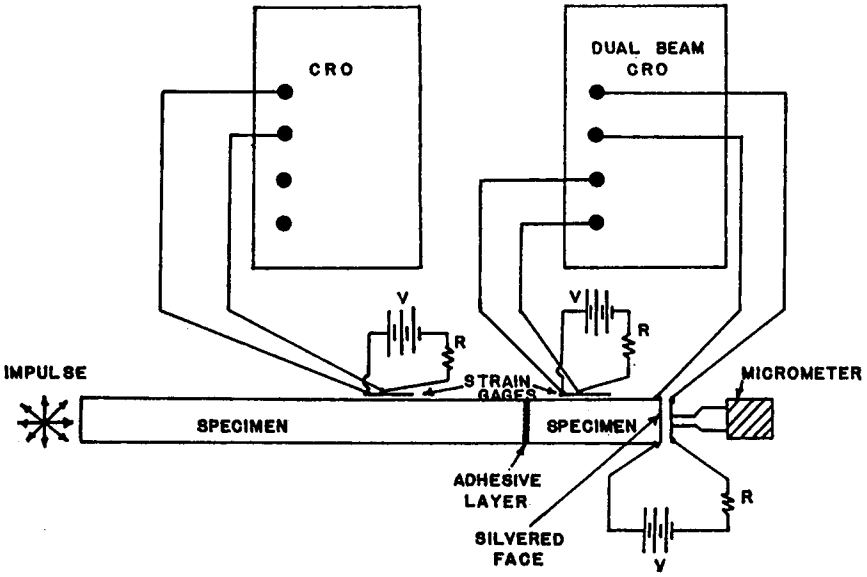


Fig. 15. Adhesive joint-specimen configuration.

An extension of the stress wave technique to elevated temperature studies is not nearly as simple as the room temperature configuration. Since plasticity effects may become operative at high temperatures one would expect attenuation of the wave to occur for this case. Since it is possible to use suitable lateral capacitative transducers in conjunction with the end displacement transducer, accurate monitoring of the traveling wave over the relatively short critical failure distances may provide sufficient data for an accurate elevated temperature tensile strength study. An elevated temperature scheme is illustrated in Figure 13.

Finally, stress wave methods should not be overlooked for possible application glass reinforced plastics strength studies as well as possible studies on the bonding characteristics of adhesive joints.

At room temperature, experiments with glass reinforced plastics could be performed in much the same manner as the brittle ceramic bars. A typical experimental setup is illustrated in Figure 14. Since GRP is not homogeneous or isotropic the effects of attenuation and dispersion would be more pronounced than in the case of the ceramics. Nonetheless such studies could provide useful information on the strengths of glass fibers as well as the mechanism of delamination between the glass and resin materials.

The dynamic bond strengths of adhesives can be investigated using the stress wave method shown in Figure 15. For this case high strength brittle bars with lapped ends could be cemented together with a thin layer of adhesive to serve as the test specimen. Strain gages on each portion of the specimen could be used to evaluate the reflection and refraction effects at the bonded boundary. As discussed earlier the transduced free end dis-

placement can be used to obtain the incident (and therefore reflected) stress-time pulse, as well as the tensile strength of the bonded joint.

Any research program of the scope described must be the result of a concerted team effort. It is with considerable pleasure that we acknowledge the contributions of Messrs. J. Anderson, J. Cistaro, R. M. Chaney, and R. Wolf, all of the Mechanics Research Division. Without their diligent efforts performance of the reported research would have been impossible. We would also like to thank Dr. J. W. Dally, Assistant Director of Mechanics Research, who suggested the reported stress wave techniques and provided guidance and encouragement throughout our research. Special credit is due the Ceramics and Graphite Branch of Materials Central who sponsored the reported research.

## References

1. Aeronautical Systems Division, *Studies of the Brittle Behavior of Ceramic Materials*, Technical Documentary Report No. ASD-TR-61-228, Wright-Patterson Air Force Base, Ohio, April 1962.

2. Bortz, S. A., *J. Am. Ceramic Soc.*

3. U. S. Naval Ordnance Laboratory, NAVORD Report 6735, May 1960.

4. Smiley, W. D., et al., "Mechanical Property Survey of Refractory Non-Metallic Crystalline Materials and Intermetallic Compounds," WADC Technical Report 59-448.

5. Kingery, W. D., and J. Pappis, *J. Am. Ceramic Soc.*, **39**, 64 (1956).

6. Folweiler, R. C., *Creep Behavior of Pore-Free Polycrystalline Aluminum Oxide*, General Electric Research Laboratory, Report No. 60-RL-2590M, December 1960.

7. Timoshenko, S., and J. N. Goodier, *Theory of Elasticity*, McGraw-Hill, New York, 1951.

8. Kolsky, H., *Stress Waves in Solids*, Clarendon, New York, 1953.

9. Kolsky, H., "Fractures Produced by Stress Waves," *Fracture*, The Technology Press of MIT, Boston, 1959.

## Résumé

On discute des techniques employées pour étudier la rupture cassante dans le domaine de vitesse d'élongation de $10^{-7}$–$10^{1}$ in/in/sec et à des températures de 75 à 1800°F. On présente des techniques destinées à accomplir une force d'élongation uniaxiale dans des barres prismatiques au moyen d'une méthode d'onde de force réflechie à des vitesses d'élongation allant jusqu'à $10^{3}$ in/in/sec, à température de chambre et à des températures élevées. Les résultats des effets mentionnés ci-dessus dans la flexion et la vérification expérimentale de l'historique de la position de la force par rapport au temps pour la technique de l'onde de force sont présentés ainsi que des explication théoriques applicables. On décrit des applications des techniques décrites ci-dessus à un spectre plus large de matériaux cassants et semi-cassants.

## Zusammenfassung

Methoden zur Untersuchung des spröden Brüches über einen Verformungsgeschwindigkeitsbereich von $10^{-7}$ bis $10^{1}$ in/in/sec und bei Temperaturen von 75° bis 1800°F werden diskutiert. Möglichkeiten zur Erzielung einer einaxialen Zugspannung in prismatischen Stäben über eine Spannungswellenreflexionsmethode bei Verformungsgeschwindigkeiten bis zu $10^{3}$ in/in/sec bei Raum- und erhöhten Temperaturen werden gezeigt. Ergebnisse der oben erwähnten Einflüsse auf Biegung, und experimentelle Verifizierung der Spannung-Zeit-Lage-Vorgeschichte für die Spannungswellenbeanspruchungsmethode werden zusammen mit anwendbaren theoretischen Erklärungen gegeben. Die Anwendung der oben angegebenen Verfahren auf einen grösseren Bereich spröder un halb-spröder Stoffe wird beschrieben.